Article Identifier
DOI: 10.22032/dbt.58913
URN: urn:nbn:de:gbv:ilm1-2023isc-056:1

60th ILMENAU SCIENTIFIC COLLOQUIUM
Technische Universität Ilmenau, 4 – 8 September 2023
URN: urn:nbn:de:gbv:ilm1-2023isc:1

Characterization of plastic-metal hybrid composites joined by means of reactive Al/Ni multilayers – evaluation of occurring thermal regime

Glaser, M.[1]; Matthes, S.[2]; Riegler, S.S.[3]; Hildebrand, J.[1]; Bergmann, J.P.[1]; Schaaf, P.[2]; Gallino, I.[3].

[1] Production Technology Group, Department of Mechanical Engineering,
Institute of Micro and Nanotechnology MacroNano®,
Technische Universität Ilmenau, Gustav-Kirchhoff-Platz 2, 98693 Ilmenau, Germany;

[2] Chair Materials for Electrical Engineering and Electronics, Institute of Materials Science and Engineering, Institute of Micro and Nanotechnology MacroNano®,
Technische Universität Ilmenau, Gustav-Kirchhoff-Strasse 5, 98693 Ilmenau, Germany;

[3] Chair of Metallic Materials,
Universität des Saarlandes, Campus C6.3, 66123 Saarbrücken, Germany

ABSTRACT

Present challenges in material science and joining technology are ever more subject to the desire for lightweight construction and engineering. Plastic-metal composites are suitable material combinations but also require the development and investigation of appropriate joining technologies. A particularly promising approach is the application of reactive multilayer foils. As an innovative method, these foils provide the possibility of flexible and low-distortion joining of dissimilar materials. The underlying reaction mechanism offers fast exothermic reaction propagation with well-known exothermic power output while the energy source is introduced directly into the joining zone. In this work, hybrid lap joints between semi-crystalline polyamide 6 and structured austenitic stainless steel X5CrNi18-10 were joined using reactive Al/Ni multilayer foils. The self-propagating reaction provides immediate temperatures that are well above the melting point of used plastic but decays rapidly after only a few milliseconds. To support ongoing investigations regarding composite formation, analysis of occurring thermal regime is in the focus of this work. Conducted experiments are supported by accompanying thermal simulation in ANSYS Workbench. Besides the estimation regarding sensitivity of thermal material parameters the evaluation of formed melting zone and resulting thermally influenced area is a central topic.

Index Terms - hybrid joints; reactive foils; self-propagating reactions; transient thermal simulation.

1. INTRODUCTION AND STATE OF THE ART

Current challenges in material science and joining technology are ever more subject to growing demands of lightweight construction and engineering. The need for new material composites is driven by ongoing developments in areas such as e-mobility and alternative vehicle drives, energy efficiency in buildings and machinery, as well as improved approaches in material recycling [1,2]. Particularly suitable material combinations for a variety of applications are hybrid plastic-metal composites, as they offer high load-bearing capacity and at the same time substantial reduction in weight. However, unequal material pairings, especially regarding dissimilar chemical and physical properties also require development and investigation of suitable joining technologies. Already established joining methods such as mechanical joining based on additional elements like screws or rivets are quite often subject to uneven load distributions, while glue based adhesive joining requires long hardening times and surface preparations. Widely applied thermal joining methods such as heat conduction joining by laser or resistance welding allow a direct connection of the materials but are subject to an increased thermal load of the joining partners and offer only a limited component-specific freedom of design [3–5].

A promising alternative is represented by the application of "reactive multilayer systems" (RMS) or reactive multilayer foils. As an innovative method, these foils provide the possibility of flexible and low-distortion joining of dissimilar partners. The underlying reaction mechanism of so called "self-propagating high-temperature synthesis" (SHS) offers fast exothermic reaction propagation with well-known exothermic power output. Due to short-term and localized application of thermal energy, requirements for welding temperature, pressure and time are reduced considerably [6–9]. Preceding work demonstrates that the temperature-time regime provided by self-propagating reactions can be applied not only to micro-scale applications like bonding of micro-electro-mechanical systems (MEMS) [10–12] but also to macro-scale applications like soldering and brazing joints of various metals and alloys [13–15]. In part, published work also involves asymmetrical joints in which the joining partners differ significantly in their thermomechanical properties [16–19]. In Leifert et al. application of reactive Ni/Al foils for similar joining of polyamide 6 (PA6) in lap joint condition is investigated. The symmetrical joining partner arrangement with low thermal conductivity behavior hinders the dissipation of released thermal energy. The melting temperature of the thermoplastic material is exceeded for approximately 25 ms at the contact surface to the reactive foil [16]. In a recently published paper hybrid lap joints between semi-crystalline polyamide 6 and austenitic stainless steel by means of reactive Al/Ni multilayer foils is investigated. The crack formations identified for this type of foil allows penetration of the foil interface with plastic and thus have a positive effect on the overall composite. The occurring crack formation is dependent on a previously introduced structuring in the metal surface [19].
Next to experimental work, accompanying numerical modeling, in particular for asymmetric joining arrangements, is currently required in more detail. Majority of published studies is based on assumptions to estimate released thermal energy defined by Mann et al. and Jayaraman et al. [20,21]. Accordingly, the physical process of shs-reaction is divided into thermal conduction along propagation direction and heat generating atomic diffusion along the layer structure. Subsequent work extends these approaches to analytical assumptions of reaction front velocity and/or released energy as a function of multilayer-specific parameters including initial composition, coefficient of atomic diffusion as well as bilayer thickness [22–25]. Another approach, aims to model the shs-process based on molecular dynamics approach (MD). Via atomic-scale modelling the mechanisms of non-isothermal processes like phase transformations or premixed interlayers are simulated [26,27]. In all cases, comparative evaluation of simulation and experimental studies is limited to microelectronic joining applications such as chip and wafer bonding [28–31] as well as metal-to-metal solder joints [32–36]. In these studies, the focus is on the simulation of shs-reaction and its influence. Here, joining partner arrangements can only be related to relatively small volumes or bonding lengths (< 1 mm), as more realistic larger joining partner arrangements would be to computationally intensive.
The thermal regime during joining of asymmetric material pairings such as plastic-metal hybrid joints with reactive multilayers is currently only insufficiently investigated. Therefore, in the context of this work, lap joints between semi-crystalline polyamide 6 (PA6) and pre-structured austenitic stainless steel X5CrNi18-10 (EN 1.4301) were joined using reactive Al/Ni multilayer foils. Performed joining tests are accompanied by temperature measurements at the foil-plastic interface. The reactive multilayer offers a stable self-propagating reaction with a front velocity of up to 8.5 m/s and maximum temperatures well above the melting point of used plastic. Corresponding heating rates of more than 10^6 K/s prove that the maximum temperature is immediately present, but decays rapidly after only a few milliseconds as a result of already fully completed reaction. To support ongoing investigations regarding composite formation, analysis of occurring thermal regime is necessary. For comparative assessment of thermal behavior, conducted experiments are supported by accompanying transient thermal simulation in ANSYS Workbench. A macroscopic model is derived that corresponds to the experimental joining arrangement in terms of geometric characteristics. Considering computational effort, thermal reaction properties are modeled as moving heat source within the joining arrangement. The reaction behavior is simulated using Birth&Death elements which are activated with corresponding thermal properties at specific points of time depending on their geometric position. Experiment as well as numerical analysis confirm that the melting temperature of the plastic material was exceeded for only a few milliseconds. Therefore, the formed melting zone and the resulting thermally influenced area in the plastic are very small. In addition, there is a high dependence of the thermal regime according to the thermal material parameters of the composite partners. A corresponding sensitivity analysis is performed based on resulting melting zone characteristics of thermoplastic material.

2. MATERIALS AND METHODS

Hybrid joints of high-alloyed steel and polyamides are of particular interest for industrial applications and are also frequently investigated using alternative thermal joining processes [37–39]. Based on previous work, the combination of thermoplastic polyamide 6 (PA6) and austenitic steel of type X5CrNi18-10 (EN 1.4301) joined by means of reactive multilayer foils is likewise chosen. It is expected that the mechanisms of heat dissipation have a significant influence on the temperature-time regime.

Reactive multilayer system:
Reactive multilayers of type Indium-NanoFoil® (Indium Corporation, Clinton, NY, USA) in the commercially available total foil thickness of 40 µm and 60 µm are used. According to the manufacturer's specifications, these multilayers have an approximately equimolar stoichiometry (atomic ratio 1:1 - Ni(V):Al; bilayer thickness 50 nm). The supplier adds a small amount of vanadium for manufacturing reasons. Negative impact on the reaction characteristics are not expected [6,40–42]. In the associated data sheets 1050 - 1250 J/g as enthalpy of reaction is specified which was confirmed by our calorimetric measurements shown in Figure 1. Under relatively slow heating rates, the DSC process corresponds to multiple solid-state reactions. However, determined enthalpies can also be used for assumptions regarding shs-reactions, that follow ignition as in [43]. Therefore, we can assume that the released thermal energy results from the exothermic conversion of Ni/Al to the final product NiAl. As consequence of ignition, the convective motion in the solid-liquid mixture enables a complete reaction following similar mechanisms described in refs. [44–49]. The foils used in this study have an additional approximately 1 µm thick brazing layer of the InCuSil-type (for specific alloy composition refer to [8,14,50]). The thermophysical properties of these commercial foils are listed in Table 2.

Metal joining partner:
Based on previous experience in the field of heat conduction joining, the high alloyed steel of type X5CrNi18-10 (EN 1.4301 / AISI 304) has proved particularly suitable for joining hybrid plastic-metal joints, as the alloy constituents promote material adhesion to polar plastics [51–54]. With an average content of 18 % chromium and 10 % nickel, this is a relatively soft, slightly-ferromagnetic austenitic steel (proportion of ferrite 5-10 %). It is characterized in particular by good corrosion resistance and is used in a wide variety of application areas. In the as-delivered condition the steel has a cold rolled surface of type 2B according to EN 10088-2. Alloy components are listed in Table 1. Thermophysical properties required for thermal simulation are listed in Table 2.

Table 1: Alloy elements of steel EN 1.4301 added to iron as per supplier's specification. Data in wt%.

C	Cr	Ni	Si	Mn	P	S	N
≤ 0.07	17.5 – 19.5	8.0 – 10.5	≤ 1.0	≤ 2.0	≤ 0.045	≤ 0.015	≤ 0.1

Thermoplast joining partner:
In this work, the semi-crystalline thermoplastic material polyamide 6 is used. Next to typical material properties as a result of the crystal modifications or morphology described in basic literature [55–58], the strong polarity of the material need to be mentioned. Accordingly, hydrogen bonds enable adhesive mechanisms to metal partners. However, the material is also subject to an increased affinity for water absorption. The thermoplastic material was supplied under specification of compliance with certain material properties according to the standards DIN EN ISO 527 and DIN 53765 labeled as “natural”, meaning it does not contain any other specific additives. To maintain user-oriented process conditions, the material was stored for several weeks at constant ambient conditions (room temperature constant at 21 °C, humidity 40 - 60 %). Common saturation with water to a maximum content of up to 3 percent according to this material must be assumed. Required material cutting is performed exclusively using dry shearing tools. For thermal joining, the melting and solidification interval of the thermoplastic material is of particular relevance. In order to determine these for the used plastic material differential scanning calorimetry (DSC) at a heating rate of 10 K min^{-1} under nitrogen atmosphere was performed (see Figure 1). The melting interval was determined to be 192 to 238 °C. The solidification interval during cooling has been measured within the range of 183 to 160 °C. According to the material data

sheet, the average melting temperature of 225 °C can be confirmed and can be used as a threshold value to be considered for subsequent analyses.

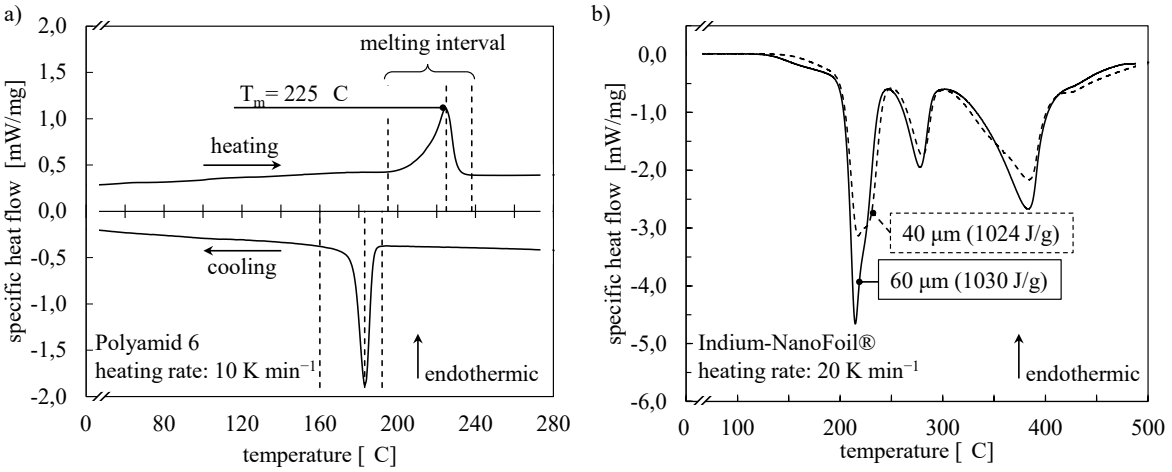

Figure 1: DSC measurements of a) the plastic material PA6 and b) reactive multilayer foils NanoFoil® with total thickness of 40 µm and 60 µm, indicating the heat released during reaction.

Table 2: Comparison of thermophysical parameters based on data sheets and literature [33–35,59–61] (values apply to room temperature).

material property	symbol	unit	RMS foil NiAl (reacted)	plastic PA6	steel EN 1.4301	copper CW004A
density	ρ	kg/m^3	5650	1130	7900	8930
heat capacity	c_p	J/(kg·K)	830	1700	470	386
thermal conductivity	λ	W/(m·K)	152	0.33	15	394
melting temperature	T_m	°C	1638	225	1420	1083
reaction temperature	T_{react}	°C	1350 -1500	-	-	-

Measurement devices for characterization:

Measurement and analysis equipment used in this publication is listed below. Device-specific settings are mentioned in the following sections at the corresponding passage.

A universal testing machine of type Hegewald & Peschke Inspekt 1455 - 20 kN is used for joining. A customized device consisting of a suitable platform and press stamp for the test specimen arrangement was developed. To compensate possible melt expulsion or lateral relaxation, the system is equipped with pretensioned springs (linear characteristic stiffness - spring rate c = 1750 N/mm).

The temperature in the compound is determined by tactile measurement using thermocouples of type K with diameter 0.1 mm. As measuring system a Devetron Dewe5000 with associated measuring card module DAQP-THERM (sample rate 3 kHz) is used.

Geometric structures and surface profiles, are evaluated based on optical measurements via laser scanning microscope (LSM) of type Olympus OLS4100 (magnification levels 20x and 50x).

Reflected light microscopy was carried out with a microscope of type Zeiss AxioScope.A1 and an additional camera of type AxioCam ICc3.

Differential Scanning Calorimetry (DSC) of thermoplastic material was performed with calorimeter of type Netzsch DSC 204 F1 Phoenix (controlled heating rate: 10 K/min, nitrogen atmosphere).

DSC calorimetric measurements of reactive multilayer foils were performed with a power-compensated Perkin Elmer Differential Scanning Calorimeter 8000 using Al pans at a constant high-purity Ar-flow (99.99 mol%) of 20 mL/min. Samples were heated continuously from 323 to 873 K at a constant rate of 0.333 K/s. A second run with reacted material under identical conditions allows the baselines subtracted from the observed first up-scan. Calibration was performed by measuring melting temperatures and enthalpies of standard metals In and Zn. For better signal-to-noise ratio, a multilayer stack of foils was placed in the Al pan.

3. EXPERIMENTAL SETUP

The used bonding arrangement is shown in Figure 2. A thickness of 1 mm for the metallic joining partner as well as 2.0 mm for the thermoplastic material was chosen while in length and width, the dimensions are equal for both types of materials at 70x10 mm. The overlap area for joining is 10x10 mm. The materials were cut dry and without additional heat input using metal cutters. Subsequent edge processing was omitted. Before inserting the reactive multilayers into the joining zone, they were cut to size of 13x10 mm, which allows one-sided accessibility for ignition (performed by electrical contact – DC 10 V / 150 mA). A joining pressure applied by means of a square press stamp ensures that the energy provided by the reaction of the multilayers can be reliably introduced into the joining partners. The applied joining pressures vary from 10 to 50 MPa with fixed increments of 10 MPa.
The metal surface is pre-structured by means of a laser device (pulsed fiber laser RofinPowerLine F20, wavelength λ = 1064 nm, settings: average power: 16 W, pulse frequency: 25 kHz, velocity: 200 mm/s; number of crossings: 3; line distance: 500 µm). These settings and corresponding geometric structure parameters width, depth as well as resulting aspect ratio refer to previous work and experience in the field of heat conduction joining. Laser scanning microscope measurements allow the estimation of resulting structural geometries. As shown in Figure 2, linear groove structures are introduced into the metal surface orthogonal to the subsequent reaction front direction. The structures have an average width of approximately 60 µm and depth of up to 20 µm. The generated structures are evenly spaced at 500 µm intervals and exhibit continuous elevations due to the melt pool ejection corresponding to the pulsed laser process. Accordingly, there are a large number of undercuts and indentations into which molten plastic can penetrate. In addition to the resulting possibility of mechanical clamping, this surface preparation also aims to enable an improved cohesive bond. Due to relatively high alloying contents of chromium and nickel in the steel, a particularly high proportion of oxides is to be expected in the metal surface, which are particularly well suited for joining with plastics. Impurities and contaminations caused by the structuring process were removed prior to joining via isopropanol ultrasonic bath.
The thermal regime during joining of asymmetric material pairings such as plastic-metal hybrid joints with reactive multilayers is currently only insufficiently investigated. For this reason, the joining tests carried out in this work are accompanied by an additional tactile in-situ temperature measurement. Thermocouples of type K with a wire diameter of 0.1 mm and measurement resolution of 3 kHz were used. They were positioned in the foil-plastic interface in the center of the joining area.

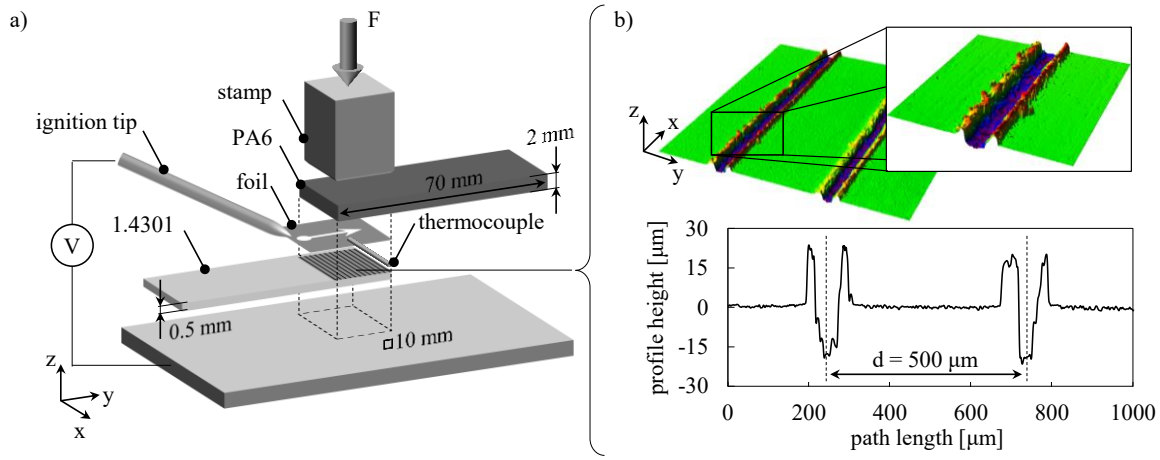

Figure 2: a) Joining setup arrangement; b) LSM measurement of structured metal surface.

4. SIMULATION SETUP

As shown in the state of the art, previous analytical and numerical models attempt to derive a prediction of velocity or thermal energy release based on specific characteristics such as material composition and bilayer thickness. These approaches show very good results, but have to be reduced to thin film systems within relatively small composite geometries in order not to exceed a certain amount of computational effort. For macroscopic joining applications, it is therefore attempted to represent the reaction in terms of a simplified propagating heat source, as a function of time and position in propagation direction. The

attempt is to reproduce the real reaction sufficiently well in terms of its thermal properties, without relying on the representation of the diffusion reaction itself. The simulations are carried out in the simulation environment ANSYS Workbench.
A schematic representation of the simulation model regarding model geometry and its boundary conditions as well as the used concept to recreate the moving heat source is shown in Figure 3. According to the geometric dimensions of experimental setup, an overlap length of 10 mm was modeled. To avoid singularities at work piece edges, an excess length of 1 mm was selected on both sides, where the generated thermal energy can dissipate into the substrate partners. The substrate thickness was set to 1 mm for both joining partners. This is legitimate, since corresponding preliminary tests confirm that the thermal properties of the plastic in particular, but also of the metal, do not cause any further influence on the temperature behavior at even larger material thicknesses. Clamping devices are therefore also omitted. According to experiments, the multilayer thickness is 40 µm and 60 µm, respectively.
The mesh consists of square elements of type "solid90" with an edge length of 0.1 mm in propagation direction (y-axis). For the reactive foil the element size in z-direction corresponds to the used film thickness. Thus, the element size is significantly larger than the bilayer thickness and metallurgical properties such as composition variation across the thickness, defects, as well as the phase evolution are not considered. The meshing of the joining partners in z-direction is achieved by means of an increase factor of 10 %. With a total number of 30 in z-direction, the elements have a height of 5 µm at the contact surface to the foil, which is then increased by 10 % with each further element layer. Preliminary sensitivity analyses confirm that this number of elements ensures a sufficiently high quality of the temperature curves at an acceptable computational cost. The transient thermal simulation is performed via conduction based heat transfer in solids in which resulting heat flow Q [W] results from density ρ [kg/m^3], heat capacity c_p [J/(kg·K)] and thermal conductivity λ [W/(m·K)]. Values are taken from Table 2. Temperature dependence as well as enthalpy of fusion is not considered, while radiation as well as convection is also not represented. Thermophysical properties of Ni/Al NanoFoil was assumed to be uniform in the thickness direction. The InCuSil brazing layer is not taken into account.

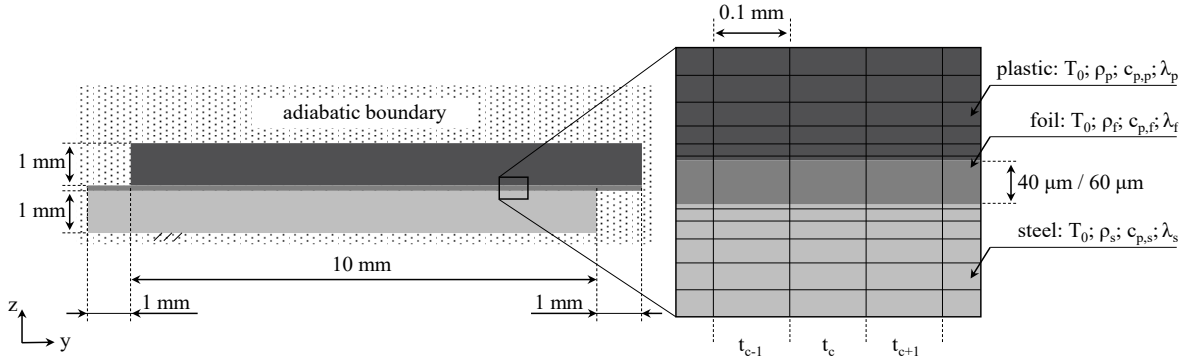

Figure 3: Schematic representation of the structure in the simulation model. Detailed image for representation of the symmetrical mesh geometry. Sketch not true to scale.

The replication of reaction front propagation is performed using the approach of Birth&Death elements via additional coding in Ansys Parametric Design Language (APDL). According to the procedure shown in Figure 3, elements are activated at the currently considered time step t_c with the defined amount of heat 1100 J/g (see chapter 2) as well as material specific properties. In the following subsequent simulation steps, these elements remain active, generate no additional heat, but conducts their own heat as well as the heat generated by subsequent elements. The amount of generated thermal energy is considered to be constant over the foil thickness. Preliminary tests showed that simultaneous activation of the following element without any own heat generation prevents the occurrence of thermal singularity. Based on element size in propagation direction a simulation time step size of 0.012 ms was defined resulting in a simulated constant front velocity of 8.33 m/s (consistency with free-standing measured velocity and literature values (for example see [23,62]). A time-dependent solver with sub-step-based division of time steps is used. After the reaction is completed, the above-mentioned time step size is maintained up to a total simulation time of 0.1 s. The simulation then proceeds in coarser time steps until the final simulation time of 1 s is reached.

5. RESULTS AND DISCUSSION

5.1 Experimental results on temperature regime

The results described here were carried out in association with a previously published paper [19]. The aim of these tests is to derive joining parameters for which the surface wetting is as optimal as possible as a function of melt quantity, foil thickness and thermal properties of the joining partners. Joining tests and obtained results confirm that a hybrid plastic-metal bond with reactive multilayers is indeed possible. Figure 4 illustrates cross-section micrographs of specimens joined at different joining pressure settings. Volume reduction of the multilayer during the reaction leads to stress and resulting crack formation in the immediate area of metal surface structuring. Molten plastic as a result of the reaction heat can penetrate these interface openings and form a bond with the metal joining partner. The possibilities for formation of structural filling and thus also the final resulting bond strength depend highly on initial joining pressure. Accordingly, a certain amount of minimum joining pressure is required to ensure not only contact and resulting melting of the plastic but also the penetration of the foil interface. However, if the initial joining pressure is too high, the still molten reactive multilayer will be pressed into the substrate structures and interferes with structure filling. As a result, the joint is weakened.

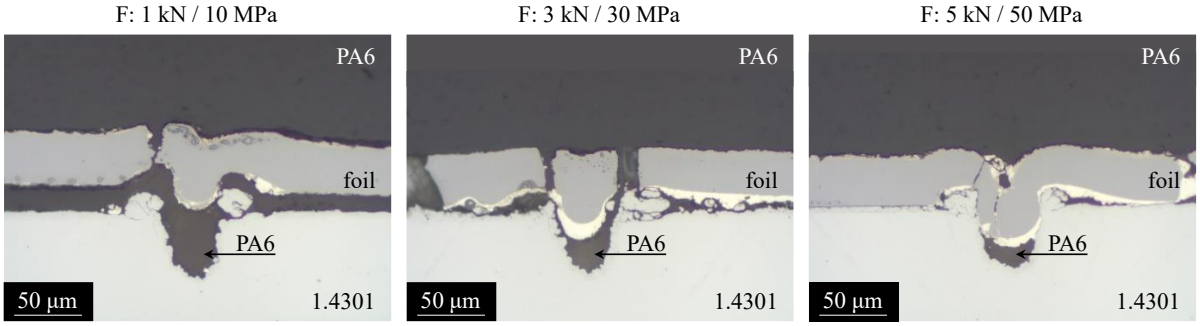

Figure 4: Cross-section of plastic metal joints. The foil ruptures in structure-near area. High dependency on structure filling and joining pressure with residual plastic in all structures.

Plastic residues could be detected in the metal structures for all performed parameter combinations. Therefore, it can be assumed that despite the relatively small amount of reactive multilayer material compared to the overall composite, the ratio of heating and cooling rates is sufficient to not only melt the plastic, but also to keep it in the molten phase for a sufficiently long period of time in order to create the described composite. In addition to maximum joint strength, compound formation mechanisms and the resulting failure behavior, it is thus necessary to estimate the thermal regime occurring during the joining process. For this purpose, the performed joining tests were additionally accompanied by temperature measurements. By using tactile thermocouples directly inserted centered in the foil/plastic interface, the temperatures occurring directly in the joining zone were measured. To ensure optimal contact, an initial joining pressure of 30 MPa was applied. Both foil variants of thickness 40 µm and 60 µm were measured. For statistical validation, each combination was repeated five times. For comparison three measurements are shown in Figure 5 each. For both foil types, the melting temperature of the plastic is significantly exceeded at the time of reaching reaction front. The amount of time for exceeding the melting temperature is 17 ms on average for 60 µm foil and approximately 8 ms on average for 40 µm foil. The heating rate, expressed as an extremely steep slope, is approximately $2.5 \cdot 10^6$ K/s for all measurements and thus in good accordance with literature data. After about 150 ms for 60 µm foil and 100 ms for 40 µm foil, the present temperature has already dropped below 100 °C and approaches values similar to room temperature after just one second. The highest measured value is 781 °C for foil variant 60 µm. On average, the maximum values for variant 40 µm are about 100 °C lower than for 60 µm. According to the generally valid assumptions of shs-reaction as well as the energy estimation by means of DSC analysis (see Figure 1), it can be assumed that both foil variants generate the same temperatures at the time of the reaction front. For thicker foil, however, it is possible to provide more thermal energy as a result of higher total mass, which in turn is reflected by the higher temperatures at the thermocouple. Another effect of lower total mass of the foil variation 40 µm is the total energy that can be estimated from the smaller area under the measurement curves.

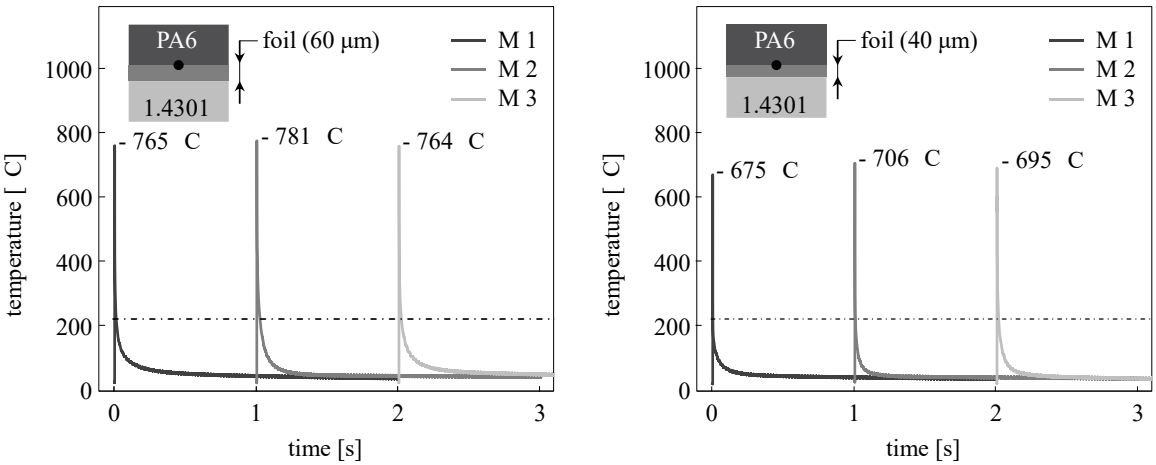

Figure 5: Measurement of occurring temperatures in the plastic/steel composite by means of tactile measurement for foil variations 60 µm and 40 µm.

It must be pointed out at this point that, as a result of the measurement procedure, a significant underestimation of the occurring maximum temperature is to be expected. Accordingly, the relationship between the inertia of thermal conduction, the period of energy generation and the total amount of available energy leads to a not inconsiderable measurement error. For this reason, it is urgent to perform a validation by means of numerical simulation.

5.2 Simulation results on temperature regime

In accordance with the procedure described in the simulation setup for mapping the reaction front by means of thermal element activation in dependence on their position, the previous described experiments were recreated. In Figure 6 the progressing evolution of reaction front and therefore resulting temperature profile in the overall composite arrangement is shown. The heat energy released by activation of the currently considered element (marked by white arrow) is passed on to the similar activated neighbor element by forward heat conduction. The activation process is repeated continuously in constant time steps over all foil elements.

With the arrival of the replicated reaction front at a considered location, the temperature increases rapidly. Due to the sub-step-based division, the maximum temperature is reached for the activated element at the end of the corresponding simulation step time. The thermal energy introduced as a mass related value leads to maximum temperatures of 1265 °C for 40 µm foil and 1278 °C for 60 µm foil respectively. An additional rising in element temperature, as a result of the activation of the following element cannot be detected. The heat extraction by the joining partners, in particular the metal side, is therefore greater than the thermal energy arriving through thermal conduction of the subsequent activated element. The absence of activated elements in front of the current front is considered to play a decisive role. Since no thermal energy can be pushed forward, the temperature does not increase with advancing position in y-direction but develops a stationary behavior for the entire reaction time.

As a result of simulation process, the temperature increases from room temperature to maximum reaction front temperature within two time steps. The heating rate thus obtained is approximately $5.2 \cdot 10^7$ K/s and is therefore 20 times higher than in the experiment. At this point it is again pointed out that it must be assumed that the experimental measurement with tactile thermocouples must be regarded as a significant underestimation of measured values. Furthermore, the maximum temperatures obtained in simulation are in good agreement with data from the literature and manufacturer specifications (see Table 2).

The individual steps illustrated in Figure 6 also show that the significantly better heat conduction properties of the metal partner have a clear effect on the asymmetric temperature profile. While heat conduction in the direction of the plastic is limited to a very narrow area, a large part of generated heat is dissipated by the metal partner. The heat extraction already shows up immediately after the reaction front has passed.

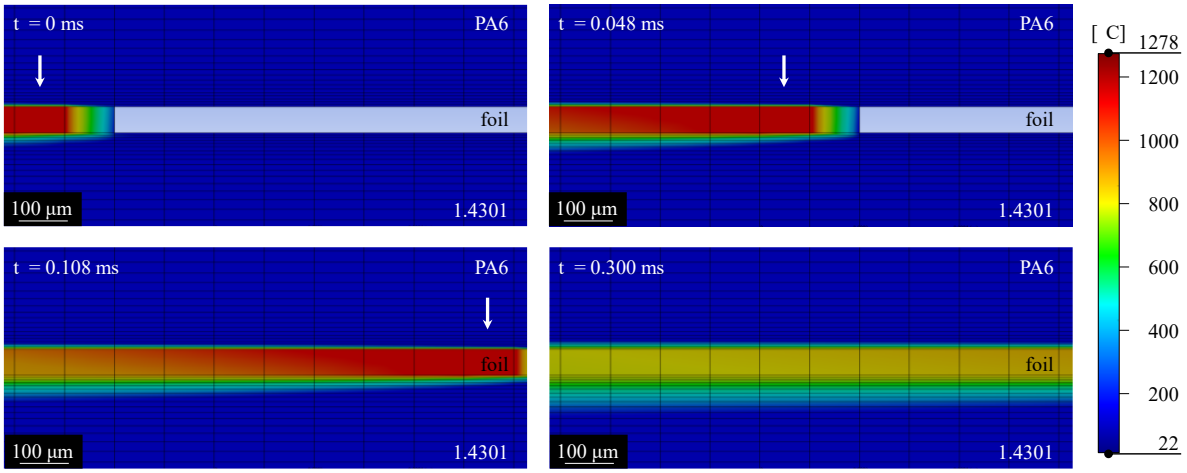

Figure 6: Stepwise visualization of reaction propagation between the joining partners. Distinct asymmetric temperature regime caused by the metal partner. Used foil thickness 60 µm.

For a better estimation of the asymmetric temperature profile caused by the different thermal properties of the joining partners, Figure 7 a) shows the temperature behavior during cooling phase at a measurement path centered in the composite over its thickness. The shown temperature curves represent different time steps during simulation starting with t = 0.01 ms, which corresponds to the time at which the currently activated element has already reached the measurement path and provides reaction temperature (at t = 0.012 ms the next element will be activated). At this point, an asymmetrical behavior of the heat dissipation can already be seen due to the thermal properties of the joining partners. At times t = 0.01 ms and t = 0.05 ms, the heat conduction of the metal partner leads to a very steep gradient within the foil layer, which straightens out with increasing time. The plastic partner shows a distinct heat-insulating effect as a result of low thermal conductivity of 0.33 W/(m·K) and therefore reduced heat dissipation.

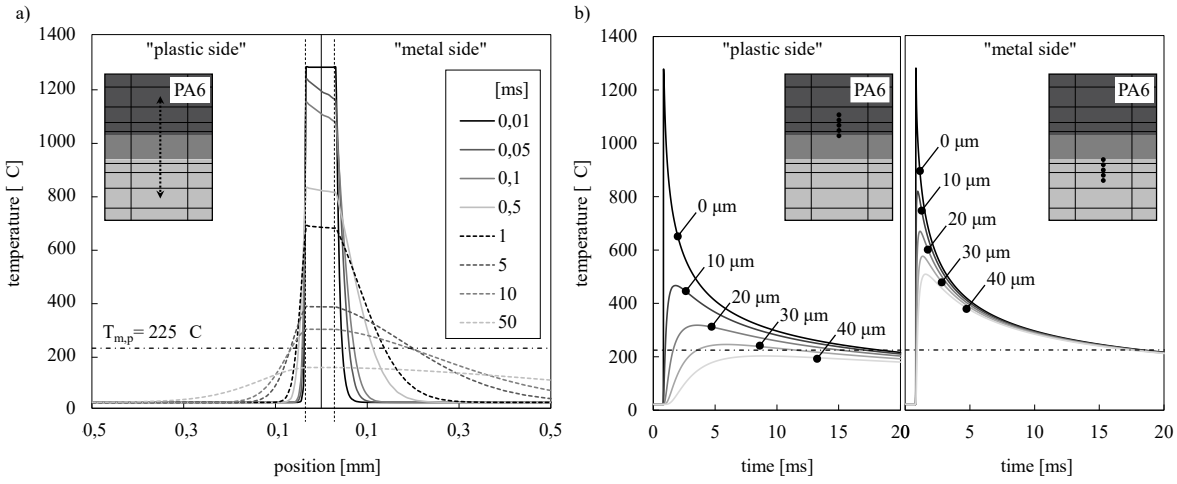

Figure 7: a) temperature behavior during cooling phase at a measurement path centered in the composite; b) spot measurement of temperature over time at fixed spatial intervals.

The melting temperature of the plastic $T_{m,p}$ as well as the width of the area in which this value is exceeded should be considered as important threshold values. While $T_{m,p}$ is exceeded almost immediately with the arrival of the front, only a maximum depth of approximatelly 35 µm (measured from the foil/plastic interface) can exceed the melting temperature due to the poor heat conduction properties of the plastic. This is also reflected in the graphs Figure 7 b). These are single point measurements, each measured starting from the foil interface and positioned at fixed distances (step size 10 µm). This representation allows a better estimation of the thermal behavior over time and is more suitable for a direct comparison with experimental temperature measurements, especially for the evaluation of the temperature regime

at the foil/plastic interface. It can be seen that the melting temperature of the thermoplast was exceeded for 9.3 ms (40 µm foil) respectively 17.4 ms (60 µm foil) at the point of contact between foil and plastic. From the simulation point of view, this is the maximum time available for wetting with molten plastic. It is also noteworthy that the increase in total mass of foil by 50% already leads to almost doubled melting time.
The asymmetry of the thermal profile shows, in addition to the unfavorable heat conduction in the direction of the plastic partners, a significantly stronger heat transport in the direction of the metallic partners multilayer and steel. A considerable amount of heat is dissipated via the metal side, which can be explained by the density of 7900 kg/m^3 which, in turn, leads to a high volumetric heat capacity, although specific heat capacity of 470 J/(kg·K) is realtively low compared to other metals like for example copper or aluminum.

5.3 Validation and sensitivity analysis

To validate previous described results, simulation and experiment have to be directly compared. Current findings indicate that, in addition to the foil thickness, the thermal regime is also significantly influenced by the used metal partner. Therefore, the temperature estimations in both experiment and simulation have been extended by adding a different metallic joining partner. The use of copper ETP (CW004A) instead of austenitic stainless steel further enhances the process-affecting thermal diffusivity behavior (material data for simulation see Table 2). A better estimation of the resulting temperature regime as well as the suitability of the simulation model becomes possible. The results are shown in Figure 8 (top row: steel with foil variations, bottom row: steel replaced with copper). The temperature measurements were carried out five times in each combination. Mean values determined from the measurements and the associated standard deviations (black dashed lines) are shown in the diagrams.

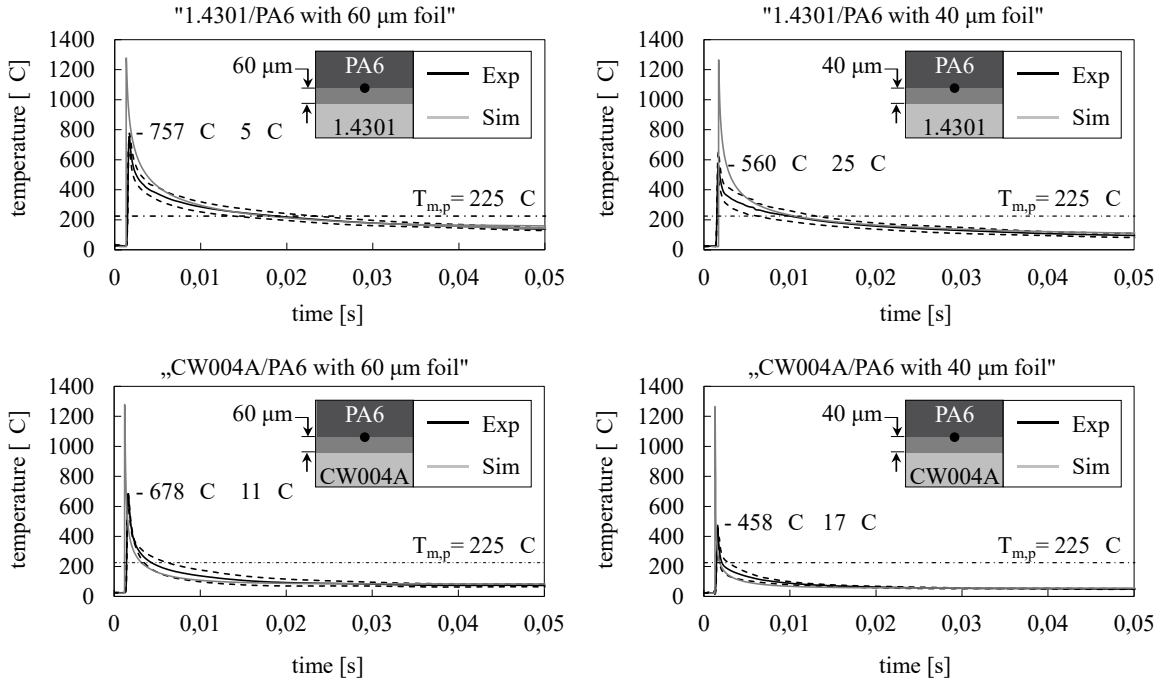

Figure 8: Temperature measurements for different material and foil combinations. Experimental scope: five measurements each. Mean value and standard deviation plotted as black lines. Simulation results shown as gray line.

From an experimental point of view, it is initially noticeable that the maximum temperature measurable by the thermocouple is significantly lower with copper partners. Once again, the assumption applies that the foil basically provides the same thermal energy, but can not be detected consistently at the thermocouple due to the measurement method, in particular contact and inertia of heat transfer. The even stronger heat dissipation caused by copper enhances this effect. At this point, the InCuSil brazing alloy on the foils should also be mentioned. Without an additional solder flux, the wetting effect is relatively poor. However, an additional increase of the heat sink effect cannot be ruled out. The temporal

resolution of the measurement system is another limiting factor when using copper, since the thermal process can only be resolved to a limited extent.
The lowest maximum temperatures are reached with copper substrate at foil thickness of 40 µm. The mean value of measured maximum temperatures is hereby 458 °C. A certain standard deviation can be seen for all curves, which begins to form in particular after the reaction front and increases in the course of cooling between 400 °C to 100 °C. For the maximum values, however, the standard deviation in the respective test setups is relatively small (see Figure 8). The measurements and the measurement procedure are thus at least qualitatively comparable, even if quantitative statements are only possible to a limited extent for the reasons already mentioned above.
Further comparison with the simulation curves shows that the maximum temperatures differ significantly between numeric and experimental results. As a consequence of the simulation concept the full amount of energy is applied to the affected element at the time of activation. An influence from the substrate can therefore only be detected in the subsequent time steps. Although the measured temperature does not reach the peak of the predicted temperature, the data curves fit quite well throughout the cooling period, in qualitative behavior as well as quantitative results. Accordingly, below 350 °C all curves are within the respective ranges of the standard deviation resulting from the experiments. As a result, the simulation model provides a very good estimation of the total time above the plastic melting temperature at the foil/plastic interface in all tested arrangements.
For the tests with austenitic steel, the simulated cooling curve lies slightly above the mean values from the experiment, while for copper there is a slight underestimation of the mean value. The ideal contact conditions as well as any deviations in the thermal properties of the joining partners, which are regarded as static, are considered as cause for this. The two tested metal materials differ significantly in their thermal properties. While density and heat capacity are still relatively close to each other, the thermal conductivity of copper $\lambda_c = 394$ W/(m·K) is 26 times higher than that of the used steel. Since the simulation model used for both material variants allows a sufficiently good estimation of the prevailing temperature profile, the question arises regarding the model's sensitivity towards changes in the material parameters. The used simplified simulation model is based on the approach of using only conductive heat without consideration of radiation or convection. Since all material parameters are assumed to be constant over temperature, the parameter sensitivity can be considered under the simplified approach of thermal diffusivity in which α [m^2/s] is equal to the ratio of thermal conductivity λ over the product of density ρ and heat capacity c_p. Furthermore, since density and capacity share the same prefactor as a product, these two values can be evaluated in the same diagram in the following.
Figure 9 shows the results of the performed sensitivity analysis (performed with a foil thickness of 60 µm). In each case, one material parameter of the joining partners was varied, while all others were kept constant. For comparison, the reference value is the so called maximum melt zone thickness ("mzt" in the diagram), i.e. the point of maximum melt temperature penetration in the plastic (measured in positive z-direction starting from the foil/plastic interface). The parameter combination used so far is selected as the starting point (see initial material values in Table 2). This results in a melt zone thickness of 39.4 µm at the simulation time t = 7.127 ms (corresponds to t = 6.327 ms after the reaction has passed the measuring point). This melt zone thickness value corresponds to the origin shown in the diagram in Figure 9. All changes in mzt value caused by parameter modifications can thus be plotted as a reference to the initial value.
The following conclusions can be drawn from the parameter sensitivity analysis. Considering the variation of density or heat capacity in the foil, an increase in these parameters leads to an increase in the resulting melt zone thickness. Since, as a result of the lowered thermal diffusivity, the foil material is not as capable of transferring heat to the metal partner, more thermal energy is available over a longer period of time, which can be released into the plastic. A different situation arises with the plastic. For this, the density and or heat capacity must be reduced to cause an increase in the melt zone thickness. The resulting better thermal diffusivity would allow more heat to be dissipated deeper into the material. The maximum value achieved during sensitivity analysis of density or heat capacity is an increase of melt zone thickness by 17 % (corresponds to an increase of 6.72 µm - leading to maximum mzt of 46.12 µm) with an increase of density or capacity of foil material by +40%. Reduction of density or capacity of plastic material by -40% would lead to nearly similar maximum values of mzt.
The metal partner behaves generally similarly to the plastic material. If the melt zone thickness is to be increased, the density and or capacity of the metal would have to be decreased. This would result in less

thermal energy being absorbed by the metal material from the foil, which in turn would provide more energy to the plastic. The sensitivity comparison of copper to austenitic steel is not yet fully possible with the analysis at this point. Although copper offers a density increase of about 13% compared to steel, it also has a reduced heat capacity of about 18%. In the linear approach of thermal diffusivity, these parameters have the same prefactor in the product, which almost compensates one another. Therefore, thermal conductivity must also be taken into account.
Considering the sensitivity of thermal conductivity, suitable effects can be observed. Thus, an increase in thermal conductivity of plastic material leads to an increase in thermal diffusivity and thus greater melt zone thickness. A maximum modification of thermal conductivity by +40% in plastic material leads to an increase of the melt zone thickness of 8 % (corresponds to an increase of 3.46 µm - leading to maximum mzt of 42.86 µm). The maximum value achieved during sensitivity analysis of thermal conductivity is an increase of melt zone thickness by 11 % (corresponds to an increase of 4.33 µm - leading to maximum mzt of 43.73 µm) with an increase of thermal conductivity of metal partner material by -40%. This shows that an increase in the melt zone thickness by changing the properties of the metal partner must be achieved by lowering the thermal conductivity, since this is the only way to reduce the temperature conduction and the resulting heat dissipation. As a result, less energy is extracted from the foil, which is then available for the plastic. This also explains the temperature behavior in the experiments with copper. The very good thermal conductivity of this metal partner generates a stronger heat sink than in the case of steel and literally extracts the temperature from the foil.
Of particular interest is the insight into the thermal properties of the foil that arises from the sensitivity analysis. While higher density and or capacity would give the foil system better ability to dissipate heat, a change in thermal conductivity introduces very little change in melt zone thickness. The cause is seen in the overall plastic/foil/steel system. In this composite, the foil has much higher values of thermal conductivity compared to the joining partners anyway. A change in thermal conductivity of the foil is not significant in view of the rather poor thermal conductivity properties of the joining partner system.

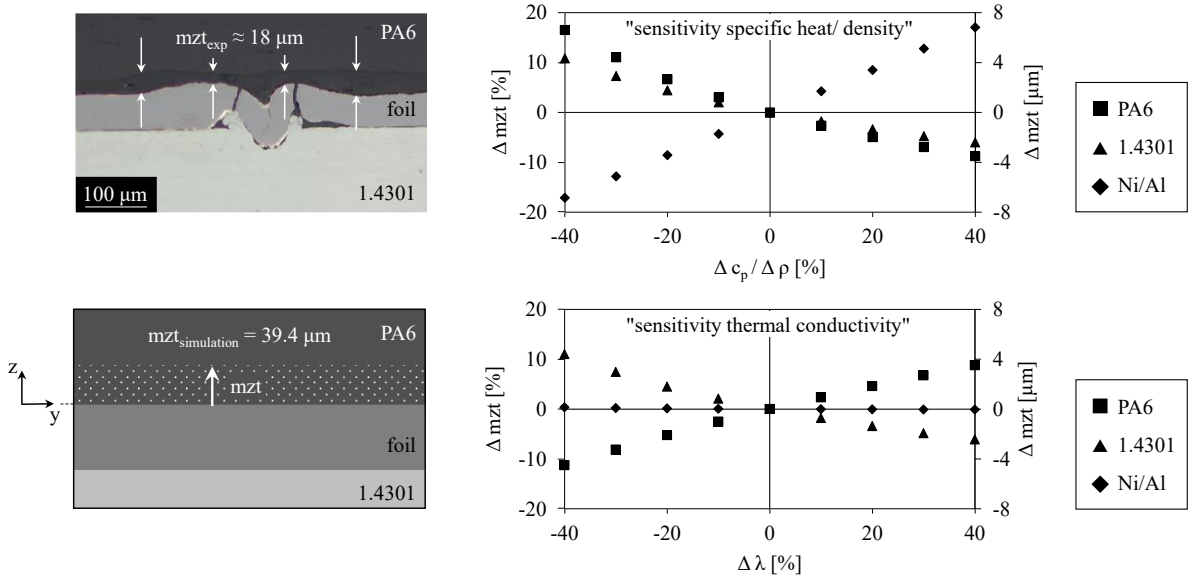

Figure 9: Determination of the sensitivity of thermal material parameters in the simulation model under consideration of linear thermal diffusivity.

The analysis of the melt zone thickness is also possible in experimentally joined samples. This is due to the effect that this melt zone can be visualized by optical reflected-light microscopy, especially in the case of semi-crystalline PA6. The reason for this is a different orientation of the material structure after resolidification and therefore optical differentiation compared to the base material. However, it is also required that the visible zone is large enough to be detected with the optical resolving capability of a reflected light microscope. While no zone can be detected for 40 µm foil, a resulting boundary layer can be visualized for 60 µm as shown in Figure 9. This zone has an average thickness of 18 µm. The reason for the deviation compared to simulation is to be seen in the joining pressure acting during the

experiments as well as the occurring melt movement. Nevertheless, the results are in a comparable scale range. The basic suitability of the simulation model is thus further verified.
In this context, the results confirm the very good suitability of the hybrid material pairing of austenitic steel and polar plastic, since the energy input of the foil, which is greatly reduced in this case anyway, is only negatively affected to a relatively small extent by the thermal properties of the metal. The hybrid material combination can be considered a rather poor thermal conductor. For future applications in hybrid macroscopic joining, it is therefore advisable to investigate other materials with relatively poor thermal conductivity, such as titanium or even ceramics, since these materials are also suitable for hybrid bonding with plastic.

6. Conclusion

The application of reactive multilayer foils for joining of plastic-metal composites is a particularly promising technology as the underlying reaction mechanism offers very fast exothermic reaction propagation with well-known exothermic power output. The thermal regime during joining of asymmetric material pairings such as plastic-metal hybrid joints with reactive multilayers is currently only insufficiently investigated. Therefore, in the context of this work, lap joints between semi-crystalline polyamide 6 (PA6) and pre-structured austenitic stainless steel X5CrNi18-10 (EN 1.4301) were joined using reactive Al/Ni multilayer foils. Performed joining tests are accompanied by temperature measurements at the foil-plastic interface. For comparative assessment of gained results, conducted experiments are supported by accompanying transient thermal simulation in ANSYS Workbench.
The obtained results show that a representation of the thermal regime in the macroscopic arrangements of hybrid plastic-metal composites is generally possible. A macroscopic model is derived that corresponds to the experimental joining arrangement in terms of geometric characteristics. Considering computational effort, thermal reaction properties are modeled as moving heat source within the joining arrangement. The reaction behavior is simulated using Birth&Death elements which are activated with corresponding thermal properties at specific points of time depending on their geometric position. Despite the model simplification, the heat transfer and its effects on the thermal process can be represented very well. Experiment as well as numerical analysis confirm that the melting temperature of the plastic material was exceeded for only a few milliseconds. Therefore, the formed melting zone and the resulting thermally influenced area in the plastic are very small. In addition, there is a high dependence of the thermal regime according to the thermal material parameters of the composite partners. A corresponding sensitivity analysis is performed based on resulting melting zone characteristics of thermoplastic material.

In summary, the results from simulation and experiment allow the following main conclusions:

- Evaluation of sensitivity in terms of material parameters confirms the assumption that for the very short time range of joining macroscopic hybrid compounds with reactive multilayers, a simplification to temperature-independent constant values is sufficient. This significantly reduces computational effort.
- In the composite, there is a thermal interaction between the metallic materials. Through thermal properties of the metallic joining partner the already asymmetric temperature regime can be further influenced.
- Measurement of the thermal profile in the joint zone by means of tactile thermocouples is subject to certain limits due to the problems of thermal conduction and measurement rate. Other methods of in-situ temperature determination must be evaluated in the future.

Funding: The study was supported by the Deutsche Forschungsgemeinschaft (DFG grants DFG BE3198/7-1 (project: 426339810), Scha 632/29 and GA1721/3-1). Support by the Center of Micro- and Nanotechnologies (ZMN), a DFG-funded core facility (DFG Scha 632/27) of the TU Ilmenau, is gratefully acknowledged.

Correspondence:
M.Sc. Marcus Glaser (marcus.glaser@tu-ilmenau.de) / https://orcid.org/0000-0003-3488-6252

REFERENCES

[1] Silva, L.R.R.; Marques, E.A.S.; da Silva, L.F.M. Polymer joining techniques state of the art review. *Weld World* **2021**, *65*, 2023–2045, doi:10.1007/s40194-021-01143-x.

[2] Zhang, W.; Xu, J. Advanced lightweight materials for Automobiles: A review. *Materials & Design* **2022**, *221*, 110994, doi:10.1016/j.matdes.2022.110994.

[3] Schricker, K.; Samfaß, L.; Grätzel, M.; Ecke, G.; Bergmann, J.P. Bonding mechanisms in laser-assisted joining of metal-polymer composites **2020**, doi:10.1016/j.jajp.2020.100008.

[4] Schricker, K.; Bergmann, J.P.; Hopfeld, M.; Spieß, L. Effect of thermoplastic morphology on mechanical properties in laser-assisted joining of polyamide 6 with aluminum. *Weld World* **2021**, *65*, 699–711, doi:10.1007/s40194-020-01048-1.

[5] Xiong, X.; Wang, D.; Wei, J.; Zhao, P.; Ren, R.; Dong, J.; Cui, X. Resistance welding technology of fiber reinforced polymer composites: a review. *Journal of Adhesion Science and Technology* **2021**, *35*, 1593–1619, doi:10.1080/01694243.2020.1856514.

[6] Adams, D.P. Reactive multilayers fabricated by vapor deposition: A critical review. *Thin Solid Films* **2015**, *576*, 98–128, doi:10.1016/j.tsf.2014.09.042.

[7] Rheingans, B.; Furrer, R.; Neuenschwander, J.; Spies, I.; Schumacher, A.; Knappmann, S.; Jeurgens, L.P.H.; Janczak-Rusch, J. Reactive Joining of Thermally and Mechanically Sensitive Materials. *Journal of Electronic Packaging* **2018**, *140*, 1–17, doi:10.1115/1.4040978.

[8] Zhu, W.; Wang, X.; Liu, C.; Zhou, Z.; Wu, F. Formation and homogenisation of Sn Cu interconnects by self-propagated exothermic reactive bonding. *Materials & Design* **2019**, *174*, 107781, doi:10.1016/j.matdes.2019.107781.

[9] Sáenz-Trevizo, A.; Hodge, A.M. Nanomaterials by design: a review of nanoscale metallic multilayers. *Nanotechnology* **2020**, *31*, 292002, doi:10.1088/1361-6528/ab803f.

[10] Hooper, R.J.; Davis, C.G.; Johns, P.M.; Adams, D.P.; Hirschfeld, D.; Nino, J.C.; Manuel, M.V. Prediction and characterization of heat-affected zone formation in tin-bismuth alloys due to nickel-aluminum multilayer foil reaction. *Journal of Applied Physics* **2015**, *117*, 245104, doi:10.1063/1.4922981.

[11] Ma, Y.; Li, H.; Bridges, D.; Peng, P.; Lawrie, B.; Feng, Z.; Hu, A. Zero-dimensional to three-dimensional nanojoining: current status and potential applications. *RSC Adv.* **2016**, *6*, 75916–75936, doi:10.1039/C6RA15897H.

[12] Matsuda, T.; Takahashi, M.; Sano, T.; Hirose, A. Multiple self-exothermic reactions for room-temperature aluminum bonding via instantaneous melting. *Materials & Design* **2017**, *121*, 136–142, doi:10.1016/j.matdes.2017.02.045.

[13] Zhu, W. Soldering Interconnects Through Self- propagating Reaction Process: A Doctoral Thesis, 2016.

[14] Rheingans, B.; Spies, I.; Schumacher, A.; Knappmann, S.; Furrer, R.; Jeurgens, L.; Janczak-Rusch, J. Joining with Reactive Nano-Multilayers: Influence of Thermal Properties of Components on Joint Microstructure and Mechanical Performance. *Applied Sciences* **2019**, *9*, 262, doi:10.3390/app9020262.

[15] Kanetsuki, S.; Miyake, S.; Namazu, T. Effect of Free-standing Al/Ni Exothermic Film on Thermal Resistance of Reactively Bonded Solder Joint. *Sensors and Materials* **2019**, *31*, 729–741, doi:10.18494/SAM.2019.2076.

[16] Leifert, A.; Mondin, G.; Dörfler, S.; Hampel, S.; Kaskel, S.; Hofmann, E.; Zschetzsche, J.; Pflug, E.; Dietrich, G.; Rühl, M.; et al. Fabrication of Nanoparticle-Containing Films and Nano Layers for Alloying and Joining. *Adv. Eng. Mater.* **2014**, *16*, 1264–1269, doi:10.1002/adem.201400196.

[17] Ma, Y.; Bridges, D.; Yu, Y.; Han, J.; Li, H.; Hu, A. Joining of Carbon Fiber Reinforced Plastic to Aluminum Alloy by Reactive Multilayer Films and Low Power Semiconductor Laser Heating. *Applied Sciences* **2019**, *9*, 1–11, doi:10.3390/app9020319.

[18] Pflug, E.; Bretschneider, J.; Leson, A. Tailored reactive multilayer systems for plastic and hybrid jointsTailored reactive multilayer systems for plastic and hybrid joints: Maßgeschneiderte reaktive Multischichtsysteme zum Fügen von Kunststoff- und Hybridverbindungen. *Joining plastics 13* **2019**, *2019*, 110–116.

[19] Glaser, M.; Matthes, S.; Hildebrand, J.; Pierre Bergmann, J.; Schaaf, P. Hybrid Thermoplastic-Metal joining based on Al/Ni multilayer foils – Analysis of the joining zone. *Materials & Design* **2023**, *226*, 111561, doi:10.1016/j.matdes.2022.111561.

[20] Mann, A.B.; Gavens, A.J.; Reiss, M.E.; van Heerden, D.; Bao, G.; Weihs, T.P. Modeling and characterizing the propagation velocity of exothermic reactions in multilayer foils. *Journal of Applied Physics* **1997**, *82*, 1178–1188, doi:10.1063/1.365886.

[21] Jayaraman, S.; Knio, O.M.; Mann, A.B.; Weihs, T.P. Numerical predictions of oscillatory combustion in reactive multilayers **1999**.

[22] Wang, L.; He, B.; Jiang, X.H. Modeling the Velocity of Self-Propagating Exothermic Reactions in Multilayer Foils. *Combustion Science and Technology* **2010**, *182*, 1000–1008, doi:10.1080/00102200903489311.
[23] Rühl, J.M.; Dietrich, G.; Pflug, E.; Braun, S.; Leson, A. Heat and Mass transfer in Reactive Multilayer Systems (RMS). Excerpt from the Proceedings of the 2012 COMSOL Conference in Milan **2012**.
[24] Kim, K. Numerical Investigation of the Self-Propagation of Intermetallic Reaction Waves in Nanoscale Aluminum/Nickel Reactive Multilayer Foils. *Korean J. Met. Mater.* **2019 Vol. 57**, 97–107, doi:10.3365/KJMM.2019.57.2.97.
[25] Baloochi, M.; Shekhawat, D.; Riegler, S.S.; Matthes, S.; Glaser, M.; Schaaf, P.; Bergmann, J.P.; Gallino, I.; Pezoldt, J. Influence of Initial Temperature and Convective Heat Loss on the Self-Propagating Reaction in Al/Ni Multilayer Foils. *Materials (Basel)* **2021**, *14*, doi:10.3390/ma14247815.
[26] Baras, F.; Turlo, V.; Politano, O.; Vadchenko, S.G.; Rogachev, A.S.; Mukasyan, A.S. SHS in Ni/Al Nanofoils: A Review of Experiments and Molecular Dynamics Simulations. *Adv. Eng. Mater.* **2018**, *20*, 1800091, doi:10.1002/adem.201800091.
[27] Schwarz, F.; Spolenak, R. The influence of premixed interlayers on the reaction propagation in Al–Ni multilayers —An MD approach. *Journal of Applied Physics* **2022**, *131*, 75107, doi:10.1063/5.0079035.
[28] Masser, R.; Braeuer, J.; Gessner, T. Modelling the reaction behavior in reactive multilayer systems on substrates used for wafer bonding. *Journal of Applied Physics* **2014**, *115*, 244311, doi:10.1063/1.4885457.
[29] Schumacher, A.; Shah, V.; Steckemetz, S.; Dietrich, G.; Pflug, E.; Hehn, T.; Knappmann, S.; Dehé, A.; Leson, A. Improved Mounting of Strain Sensors by Reactive Bonding **2021**, doi:10.1007/s11665-021-05993-w.
[30] Arlington, S.Q.; Fritz, G.M.; Weihs, T.P. Exothermic Formation Reactions as Local Heat Sources. *Annu. Rev. Mater. Res.* **2022**, *52*, 219–248, doi:10.1146/annurev-matsci-081720-124041.
[31] Yuile, A.; Schulz, A.; Wiss, E.; Müller, J.; Wiese, S. The Simulated Effect of Adding Solder Layers on Reactive Multilayer Films Used for Joining Processes. *Applied Sciences* **2022**, *12*, 2397, doi:10.3390/app12052397.
[32] Rühl, J.M. *Prozessmodellierung von Reaktiv-Multischicht-Systemen (RMS)*. -PhD thesis, 2015.
[33] Zhou, Z.; Mo, L.; Liu, H.; Chan, Y.C.; Wu, F. Study of Fusion Thickness of Tin Solder Heating by Self-Propagating Exothermic Reaction. *Journal of Elec Materi* **2018**, *47*, 7435–7448, doi:10.1007/s11664-018-6684-9.
[34] Liang, S.; Zhong, Y.; Robertson, S.; Liu, A.; Zhou, Z.; Liu, C. Investigation of Thermo-mechanical and Phase-change Behavior in the Sn/Cu Interconnects during Self-Propagating Exothermic Reaction Bonding **2020**, 269–275, doi:10.1109/ECTC32862.2020.00052.
[35] Liang, S.; Zhong, Y.; Robertson, S.; Liu, A.; Jiang, H.; Liu, C.; Zhou, Z.; Liu, C. Investigation of thermal effect on solidification in Sn/Cu interconnects during self-propagating exothermic reaction bonding. *Microelectronics Reliability* **2022**, *138*, 114654, doi:10.1016/j.microrel.2022.114654.
[36] Wang, X.; Li, M.; Zhu, W. Formation and homogenization of Si interconnects by non-equilibrium self-propagating exothermic reaction. *Journal of Alloys and Compounds* **2020**, *817*, 153210, doi:10.1016/j.jallcom.2019.153210.
[37] Jiao, J.; Xu, Z.; Wang, Q.; Sheng, L.; Zhang, W. CFRTP and stainless steel laser joining: Thermal defects analysis and joining parameters optimization. *Optics & Laser Technology* **2018**, *103*, 170–176, doi:10.1016/j.optlastec.2018.01.023.
[38] Rodriguez-Vidal, E.; Sanz, C.; Bayon, R. Hybrid joints of polymer and thin metal parts fabricated by laser technology: performance under realistic conditions. Lasers in Manufacturing Conference 2019 **2019**.
[39] Elahi M.A.; Hennico, M.; Plapper, P. The effect of temperature and joining speed on the joining quality for conduction laser joining of metals to polymers **2021**.
[40] Grapes, M.D.; LaGrange, T.; Woll, K.; Reed, B.W.; Campbell, G.H.; LaVan, D.A.; Weihs, T.P. In situ transmission electron microscopy investigation of the interfacial reaction between Ni and Al during rapid heating in a nanocalorimeter. *APL Materials* **2014**, *2*, 116102, doi:10.1063/1.4900818.
[41] Maj, Ł.; Morgiel, J.; Szlezynger, M.; Bała, P.; Cios, G. Effect of low and high heating rates on reaction path of Ni(V)/Al multilayer. *Materials Chemistry and Physics* **2017**, *193*, 244–252, doi:10.1016/j.matchemphys.2017.02.033.
[42] Maekawa, K.; Ito, S.; Namazu, T. Influence of bonded area size on cracking in reacted NiAl layer for crack-free reactive soldering. *Jpn. J. Appl. Phys.* **2020**, *59*, SIIL01, doi:10.35848/1347-4065/ab769b.
[43] Wang, A.; Gallino, I.; Riegler, S.S.; Lin, Y.-T.; Isaac, N.A.; Sauni Camposano, Y.H.; Matthes, S.; Flock, D.; Jacobs, H.O.; Yen, H.-W.; et al. Ultrafast formation of single phase B2 AlCoCrFeNi high entropy alloy films by reactive Ni/Al multilayers as heat source. *Materials & Design* **2021**, *206*, 109790, doi:10.1016/j.matdes.2021.109790.

[44] Kim, J.S.; LaGrange, T.; Reed, B.W.; Knepper, R.; Weihs, T.P.; Browning, N.D.; Campbell, G.H. Direct characterization of phase transformations and morphologies in moving reaction zones in Al/Ni nanolaminates using dynamic transmission electron microscopy. *Acta Materialia* **2011**, *59*, 3571–3580, doi:10.1016/j.actamat.2011.02.030.
[45] Trenkle, J.C.; Koerner, L.J.; Tate, M.W.; Walker, N.; Gruner, S.M.; Weihs, T.P.; Hufnagel, T.C. Time-resolved x-ray microdiffraction studies of phase transformations during rapidly propagating reactions in Al/Ni and Zr/Ni multilayer foils. *Journal of Applied Physics* **2010**, *107*, 113511, doi:10.1063/1.3428471.
[46] Gunduz, I.E.; Fadenberger, K.; Kokonou, M.; Rebholz, C.; Doumanidis, C.C. Investigations on the self propagating reactions of nickel and aluminum multilayered foils. *Appl. Phys. Lett.* **2008**, *93*, 134101, doi:10.1063/1.2994670.
[47] A. S. Edelstein; R. K. Everett; G. Y. Richardson; S. B. Qadri; E. I. Altman; J. C. Foley; J. H. Perepezko. Intermetallic phase formation during annealing of Al/Ni multilayers **1994**.
[48] Blobaum, K.J.; van Heerden, D.; Gavens, A.J.; Weihs, T.P. Al/Ni formation reactions: characterization of the metastable Al9Ni2 phase and analysis of its formation. *Acta Materialia* **2003**, *51*, 3871–3884, doi:10.1016/S1359-6454(03)00211-8.
[49] Blobaum, K.J.; Reiss, M.E.; Plitzko, J.M.; Weihs, T.P. Deposition and characterization of a self-propagating CuOx/Al thermite reaction in a multilayer foil geometry. *Journal of Applied Physics* **2003**, *94*, 2915–2922, doi:10.1063/1.1598296.
[50] Wang, J.; Besnoin, E.; Knio, O.M.; Weihs, T.P. Effects of physical properties of components on reactive nanolayer joining. *Journal of Applied Physics* **2005**, *97*, 114307, doi:10.1063/1.1915540.
[51] Szallies, K.; Bielenin, M.; Schricker, K.; Bergmann, J.P.; Neudel, C. Single-side resistance spot joining of polymer-metal hybrid structures **2019**, doi:10.1007/s40194-019-00728-x.
[52] Schricker, K.; Bergmann, J.P. Temperature- and Time-Dependent Penetration of Surface Structures in Thermal Joining of Plastics to Metals, doi:10.4028/www.scientific.net/KEM.809.378.
[53] Schricker, K.; Pierre Bergmann, J. Determination of sensitivity and thermal efficiency in laser assisted metal-plastic joining by numerical simulation. *Procedia CIRP* **2018**, *74*, 511–517, doi:10.1016/j.procir.2018.08.133.
[54] Schricker, K.; Bergmann, J.P. Temperature- and Time-Dependent Penetration of Surface Structures in Thermal Joining of Plastics to Metals **2019**, doi:10.4028/www.scientific.net/KEM.809.378.
[55] Zhang, G.; WATANABE,Hirohisa YOSHIDA,† and Tadashi KAWAI. Phase Transition Behavior of Nylon-66, Nylon-48, and Blends. *Polymer Journal, Vol. 35, No. 2,* **2003**, *2003*, 173–177.
[56] Yash P. Khanna/William P. Kuhn/William J. Sichina. Reliable Measurements of the Nylon 6 Glass Transition Made Possible by the New Dynamic DSC **1995**, 2644–2646.
[57] Khanna, Y.P.; Kuhn, W.P. Measurement of crystalline index in nylons by DSC: Complexities and recommendations **1997**.
[58] Schricker, K. *Charakterisierung der Fügezone von laserbasiert gefügten Hybridverbunden aus teilkristallinen thermoplastischen Kunststoffen und Metallen*. -PhD thesis, 2018.
[59] Martin, H. *VDI-Wärmeatlas, 11.Auflage;* Springer Berlin Heidelberg: Berlin, Heidelberg, 2013.
[60] Bonnet, M. *Kunststofftechnik - Grundlagen, Verarbeitung, Werkstoffauswahl und Fallbeispiele;* Springer Fachmedien Wiesbaden: Wiesbaden, 2016.
[61] Mueller, M.; Franke, J. Highly efficient packaging processes by reactive multilayer materials for die-attach in power electronic applications **2014**, 477–481, doi:10.1109/EPTC.2014.7028295.
[62] Schulz, A.; Bartsch, H.; Matthes, S.; Glaser, M.; Müller, J.; Schaaf, P.; Bergmann, J.P.; Wiese, S.; Gutzeit, N. Characterization of Reactive Multilayer Systems deposited on LTCC featuring different surface morphologies **2021**, doi:10.1109/EUMC.2006.281442.

